PERINATAL JOURNAL

Original Article

Perinatal Journal 2026; 34(1):62-73

https://doi.org/10.57239/prn.26.0341009

Synthesis, characterization, molecular docking and biological activity: Novel Nano graft copolymer-paracetamol drug composite as a potential treatment of breast cancer cell line (MCF-7)

Hussein H. M. Al-Masoudi[1], Mohammad N. AL-Baiati [2], Karim Akbari Dilmaghani[1]

[1]*Urmia University, Faculty of Science, Department of Chemistry, Urmia, Iran*
[2]*University of Kerbala, College of Education for Pure Sciences, Department of Chemistry, Karbala, Iraq*

Abstract

In this study, we embarked on an intriguing journey to create a groundbreaking nano graft copolymer–Paracetamol drug composite, and we eagerly assessed its anticancer potential against the MCF-7 breast cancer cell line. The creation of our nano copolymer was a result of a poly condensation reaction that cleverly combined 2.0 moles of glycerol with 4.0 moles of phthalic anhydride. We left no stone unturned in confirming its structure, utilizing an array of techniques like FT-IR, ^{1}H NMR, ^{13}C NMR, and various imaging methods including X-ray diffraction (XRD), transmission electron microscopy (TEM), and atomic force microscopy (AFM) to ensure its integrity. By further functionalizing the copolymer with 1.0 mole of Paracetamol, we crafted a nano drug composite that was subjected to the same rigorous characterization methods. We didn't stop there; molecular docking analysis was performed to dive deeper into the interactions between our composite and crucial proteins linked to breast cancer. The results were promising, revealing favorable binding interactions that hinted at a possible therapeutic mechanism at play. When we turned to in vitro cytotoxicity assays against MCF-7 cells, the results were quite remarkable—an impressive IC_{50} value of 52.46 µg/mL showcased the significant anticancer activity of our creation. These findings paint a vivid picture of the potential that our synthesized nano drug composite holds as a targeted therapy for breast cancer, setting the stage for future research and development in this vital area.

Keywords: Nano copolymer, Nano graft copolymer, Paracetemol, Drug composite, Molecular docking, Breast cancer, MCF-7 cell line, Cytotoxicity.

Introduction

Nanotechnology is a fascinating realm that involves the intricate manipulation and application of materials at the nano scale consider this: a nanometer is an astonishing one billionth of a meter (1×10^{-9} m). To put it in relatable terms, this tiny measurement is roughly 100,000 times thinner than a strand of human hair! Among the myriad of nano materials we encounter, some of the most prevalent include nanoparticles, nanotubes, and nano fibers, each boasting its own intriguing mix of physical, chemical, and biological characteristics. The emergence of nanotechnology has sparked revolutionary breakthroughs across various fields, with medicine standing out as a particularly bright beacon of progress. Here, it plays an essential role in areas such as drug delivery, diagnostics, bio sensing, and even the engineering of tissues. Now, let's shift our focus to breast cancer, which holds the somber title of the most commonly diagnosed cancer and ranks as a leading cause of cancer-related fatalities among women globally. This alarming trend is especially pronounced in developed countries like the United States. Breast cancer emerges when cells in the breast tissue begin to grow uncontrollably, forming malignant tumors. The signs can be subtle yet alarming: palpable lumps, noticeable changes in breast shape or texture, and even inverted nipples may signal the presence of this insidious disease. As the cancer advances, its cells have the potential to metastasize—spreading to nearby lymph nodes or even distant organs—making treatment a far more daunting challenge. [7,8].

In the ever-evolving world of cancer treatment, one of the most exciting avenues being explored is the use of nano carrier-based drug delivery systems. These innovative platforms are crafted to encapsulate therapeutic agents, ensuring they're delivered with pinpoint accuracy to the desired location in the body. By leveraging these tiny carriers, scientists can

Correspondence: Karim Akbari Dilmaghani, Urmia University, Faculty of Science, Department of Chemistry, Urmia, Iran, **e-mail:** K.adilmaghani@urmia.ac.ir,
Received: August 16, 2025 **Accepted:** September 1, 2025

significantly enhance how drugs are absorbed, reduce the chance of them being broken down by enzymes, and cut down on unwanted side effects that can arise when drugs stray from their intended targets. When these nano carriers reach the designated tissue, they play a pivotal role in promoting cellular uptake, ultimately releasing the active drug right at the heart of where it's needed most. Take amoxicillin, for instance—this β-lactam antibiotic, a proud member of the amino penicillin subclass, has cemented its place in the medical community as a go-to treatment for a wide range of bacterial infections. Its broad-spectrum antimicrobial prowess coupled with a solid safety profile has made it a favorite among healthcare providers. But here's where it gets particularly intriguing: recent studies have started to uncover that certain antibiotics, like amoxicillin, might possess hidden talents beyond just fighting infections. They may influence cellular pathways linked to tumor progression, sparking the possibility of repurposing these familiar drugs for a new role in the realm of cancer therapy. Isn't that fascinating? [12].

In this exciting study, we delve into the creation and analysis of a groundbreaking nano copolymer system that has been cleverly infused with amoxicillin. The copolymer itself was crafted through a poly condensation reaction between glycerol and phthalic anhydride two seemingly unassuming substances that, when combined, form a robust foundation for our innovative drug composite. Following this, we strategically attached amoxicillin, aiming to enhance the targeting capabilities of our formulation. To ensure that we properly understood the intricate details of our nano composite, we employed a variety of sophisticated characterization techniques. This included FT-IR, NMR, XRD, TEM, and AFM—each method unveiling a different layer of the structural and morphological identity of our creation. But we didn't stop there! We also conducted molecular docking simulations, allowing us to anticipate how effectively our drug might interact with proteins linked to breast cancer. To round out our investigation, we executed in vitro cytotoxicity assays, putting our composite to the test against the MCF-7 breast cancer cell line to assess its anticancer potential. This research not only adds a significant piece to the expanding puzzle of nano-enabled drug delivery systems but also highlights the promising role that antibiotic-functionalized nano materials could play in the realm of targeted cancer therapy. The implications of this work could reshape how we approach treatment strategies in the future, opening new avenues for effective interventions.

Methodology

Synthesis of nano graft copolymer

Phthalic anhydride (2.5 mol) (370gram) was dissolved in 3.7 mL of dimethyl sulfoxide (DMSO) in a 65 mL beaker equipped with a thermometer. The mixture was heated to 155°C and stirred continuously using a magnetic stirrer for 22 minutes, resulting in a colorless liquid. Subsequently, glycerol (1 mol, 92 g) was added to initiate the poly condensation reaction. To facilitate the removal of water produced during esterification, approximately 5 mL portions of xylene were gradually introduced. After an additional 15 minutes of reaction, the heating was discontinued. The reaction mixture was then poured into cold deionized water (3°C) to precipitate the product. Resulting solid was collected by filtration, washed thoroughly with deionized water, and dried at room temperature. Finally, the dried solid was pulverized to obtain the nano co-polymer as illustrated in Equation (1) [3].

Synthesis of acid chloride of nano graft copolymer

To prepare (polymer-Cl) the acid chloride derivative, take 0.6 g of the previously synthesized nano graft co-polymer was mixed with 4–5 drops of ($SOCl_2$) thionyl chloride and 6.0 mL of (DCM) dichloromethane in beaker 25 mL. The mixture was stirred magnetically on the hot billet and allowed to rest at room temperature(25C°) for Half an hour to enable initial activation. It was then heated to 65C° and maintained for two hours (120 minute) to promote acylchloride(-CO-Cl) formation. In the end , the temperature increased to 85C° and maintained for an additional (120 minute) to ensure complete conversion. The resulting nano co-polymer–acid chloride(polymer has Cl) product was collected and used in the next reaction of the synthesis [14], as illustrated in Equation 2.

Synthesis of nano drug composite

Paracetemol (1.5 g, 1.0 mol) was dissolved in 8 mL of dichloromethane (DCM) along with (0.5 mL) half

mol of triethylamine under continuous and stirring in an ice bath. This solution was slowly added to the acid chloride-modified nano co-polymer prepared in the previous step reaction (0.6 g). The resulting mixture (polymer + drug) was transferred into a beaker 50 mL containing crushed ice water and stirred thoroughly with a glass rod until the ice melted and a precipitate formed (The reaction do on the hood) .

The solid product was filtered from the water , washed of methanol , and then stirred in an ice bath for 60 minute , followed by additional stirring at room temperature(25C°) for 3 hours to complete the reaction. The obtained drug-loaded nano composite was dried and characterized accordingly [15,31], as shown in Equation 3.

Molecular docking

Molecular docking modern studies were conducted to evaluate the interaction between the synthesized nano drug composite (co-polymer & prastimol) with cancer cell breast cancer. The docking simulations of three software were carried out using PyRx software and Biovia software integrated with the (MOE) Molecular Operating Environment module. These tools enabled the prediction of binding between the protein cell cancer and nano drug delivery affinities, identification of key amino acid residues involved in drug–receptor interactions, and visualization of molecular conformations. The results provided insight into the potential binding mechanisms and biological relevance of the synthesized compound [16].

Biological activity

In 100 U/ml penicillin and 100 µg/ml streptomycin, MCF-7 human breast cancer cells were cultured in RPMI-1640 medium supplemented with 10% fetal bovine serum (FBS), 100 ml. Cells were maintained under standard conditions of pressure, temperature, and humidity in a humidified incubator at 37°C with 5% CO. Cells were passaged with trypsin-EDTA and seeded at approximately 80% confluence for experiments [3,17].

Cytotoxicity assay

The cytotoxic effect of the nano Paracetemol drug composite was evaluated using the MTT assay in 96-well plates. MCF-7 human breast cancer cells were seeded at a density of 1×10^4 cells from each well and allowed to adhere for one day . The cells were then treated with varying concentrations of the nano drug delivery composite and incubated for three day .

After treatment, the culture medium was removed, and 1*102 µL of MTT solution (2*10-3 mg/mL) to each well was added. The cells were incubated at 37 °C for 3 hours to allow formazan crystal formation. Following incubation, the MTT solution was removed, and 130 µL of dimethyl sulfoxide (DMSO) was added to dissolve the formazan crystals. The plate was shaken gently and incubated at 37 °C for an additional 15 minutes. Absorbance was measured at 492 nm using a microplate reader.

Cell viability and inhibition rate were calculated using the following formula:

$$\text{Inhibition rate} = \frac{(A-B)}{A} \times 100$$

Inhibition rate =

Where:

A = absorbance of control (untreated cells)

B = absorbance of treated sample

All experiments were conducted in triplicate.

Data analysis

Statistical analysis was performed using unpaired Student's t test in GraphPad Prism (version 6). Results are presented as mean ± standard deviation (SD) based on three independent experimental replicates. A p value <5*10-2 was considered to be of certain statistical significance [18].

Results and Discussion

Synthesis and characterization of the nano copolymer and its acid chloride

The nano-drug copolymer was successfully synthesized following the procedure described in the polymer synthesis section, which includes the reaction of glycerol with phthalic anhydride. The

resulting material was purified and characterized using different analytical techniques, including FT-IR, ^{1}H NMR, ^{13}C NMR, X-ray diffraction (XRD), transmission electron microscopy (TEM), and atomic force microscopy (AFM), to confirm the structure, morphology, and properties of the prepared nanoparticles. Spectroscopic analysis (FT-IR, NMR) The above tests confirmed the formation of ester bonds and the preservation of functional groups within the internal structure of the polymer. The conversion of the copolymer into the acid chloride derivative was confirmed by the appearance of characteristic peaks in the examination of the FT-IR spectrum, indicating successful chlorination of the terminal carboxylic acid groups in the polymer. The polymer was prepared according to the synthetic steps in Equation (1) to form the nano polymer and Equation (2). Likewise, a polymer containing chlorine in 2 was prepared to prepare the grafted nano polymer acid chloride. These foundation compounds were used in subsequent steps to conjugate with Paracetamol to form the drug-loaded nano co-polymer.

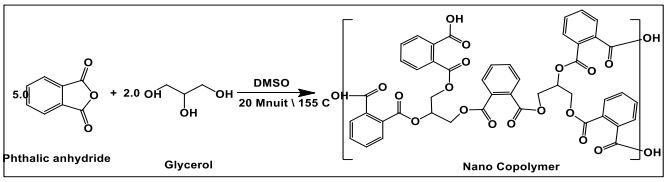

Equation 1. Synthesis of nano co-polymer

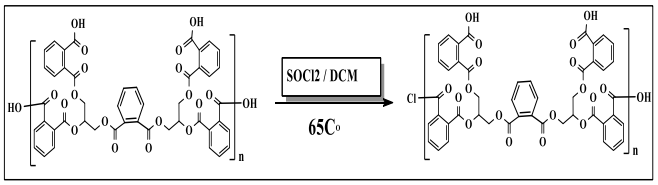

Equation 2. Synthesis of nano co-polymer acid chloride

Spectroscopic and structural characterization of nano graft copolymer

FT-IR spectrum (Figure 1) of the synthesized nano co-polymer confirmed the presence of characteristic functional groups. A broad absorption band between 3500–3250 cm^{-1} corresponds to O–H stretching vibrations of carboxylic acid groups. The aromatic sp^{2} C–H stretching vibration appeared at 3057 cm^{-1}, while the aliphatic sp^{3} C–H stretching bands were observed at 2998 and 2873 cm^{-1}. A strong band at 1760 cm^{-1} indicates the presence of ester (C=O) linkages, confirming successful esterification. Additionally, a band at 1667 cm^{-1} corresponds to carbonyl stretching vibrations, supporting the formation of the polymer backbone [19,20].

^{1}H NMR spectrum (Figure 2) of the nano copolymer (recorded in DMSO-d_6, 400 MHz) revealed distinct signals corresponding to the polymer structure. A broad singlet at δ = 13.20 ppm was attributed to the hydroxyl protons of the carboxylic acid groups. Multiple peaks between δ = 8.10–7.99 ppm and 7.75–7.68 ppm correspond to aromatic protons from various positions in the polymer framework. A quintet at δ = 2.60–2.59 ppm is assigned to methane group protons, and a doublet at δ = 2.54 ppm corresponds to methylene group protons. These results confirm the expected substitution and aromaticity of the polymer [21,22].

^{13}C NMR spectrum (Figure 3), (DMSO-d_6, 8.15 MHz) further supports the structure of the synthesized nano copolymer. Carbonyl carbon signals were observed at δ = 173.12 ppm and 169.20 ppm, indicating the presence of carboxylic and ester functionalities. Aromatic carbons appeared within the δ = 125–135 ppm range. Signals at δ = 66.8 ppm and 45.23 ppm were assigned to aliphatic carbons, specifically those in methylene and methane environments, verifying the polymer framework and side-chain structures [23,24].

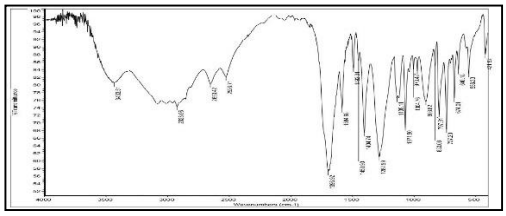

Figure 1. FT-IR spectrum of synthesis nano graft copolymer

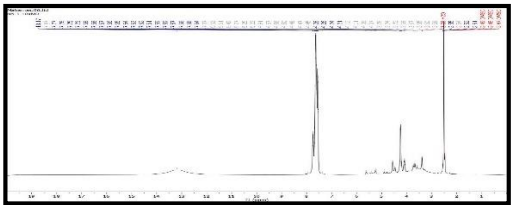

Figure 2. ^{1}H-NMR spectrum of synthesis nano graft copolymer

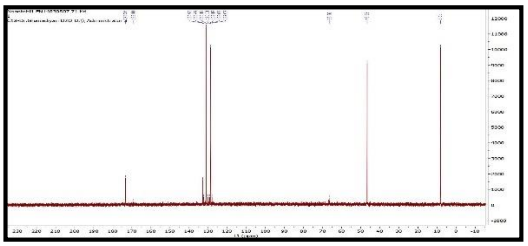

Figure 3. ^{13}CNMR spectrum of synthesis nano graft copolymer

X-ray diffraction analysis (Figure 4):

The XRD pattern of the nano copolymer displayed multiple diffraction peaks at 2θ values of 15.044°, 18.901°, 20.000°, 27.154°, 31.450°, 39.780°, 46.000°, and 47.840°. These peaks indicate a semi-crystalline nature of the material, with moderate crystallinity and minimal amorphous content. The average interplanar spacing (d_{hkl}) was calculated to be 0.569 nm using Bragg's Law:

$$n\lambda=2d\sin(\theta)$$

Where n is the diffraction order, λ is the wavelength of the X-ray source, d is the interplanar spacing, and θ is the diffraction angle [25].

The average crystallite size was determined to be approximately 57.6 nm using the Scherrer equation:

$$D= K\lambda / \beta \cos(\theta)$$

Where D is the crystallite size, K is the shape factor (typically 0.9), λ is the X-ray wavelength, β is the full width at half maximum (FWHM), and θ is the Bragg angle [26]. These results confirm the nanoscale structure and crystalline nature of the synthesized copolymer.

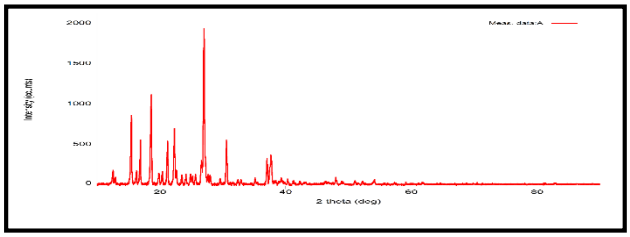

Figure 4. X-Ray spectrograph of nano polymer

Table 1. Crystals proportions and the distances of atoms in nano copolymer

2θ	θ	FWHM	D	D	D (EV.)	d(EV.)
15.044	7.5218	0.0778	52.2	0.8140	**57.6**	**0.569**
18.901	9.4505	0.0228	63.0	0.3170		
20.000	10.0000	0.0553	29.9	0.4188		
27.154	13.5770	0.0532	49.0	0.6180		
31.450	15.7250	0.0263	52.6	0.4710		
39.780	19.8900	0.0698	29.3	0.6250		
46.000	23.0000	0.0289	92.4	0.6130		
47.840	23.9200	0.0452	92.4	0.6830		

Surface morphology and topography analysis (AFM)

Figure 5 presents the three-dimensional atomic force microscopy (AFM) images of the synthesized nano copolymer, revealing detailed information about its surface morphology and particle distribution. The surface of the polymer appears uniform with a relatively consistent particle dispersion, supporting the formation of a nanoscale material.

AFM analysis confirmed that the polymer particle sizes fell well within the nanometer range, with measured diameters of approximately 57.04 nm (Figure 5a) and 23.59 nm (Figure 5b). This size distribution further validated the successful fabrication of a nanostructured material.

The roughness coefficient of the linear nano copolymer surface was calculated to be 29.72 nm, while the root mean square (RMS) roughness value was 60.65 nm, as illustrated in Figure 6. These values confirm the presence of significant surface roughness, a characteristic commonly associated with nanoscale materials. Moreover, the average particle height was recorded at 188.9 nm and 16.52 nm, further emphasizing the vertical uniformity and nanoscale thickness of the synthesized polymer.

Overall, the AFM analysis supports the conclusion

that the synthesized copolymer exhibits nanoscale dimensions, surface homogeneity, and crystalline surface features—key properties that enhance its potential application in drug delivery systems.

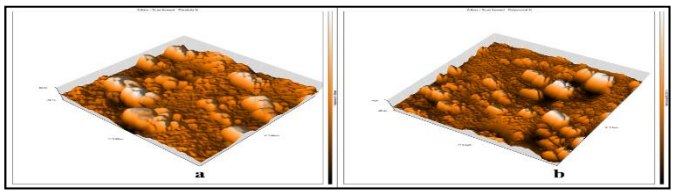

Figure 5. 3D imaging of AFM morphological of nano polymer

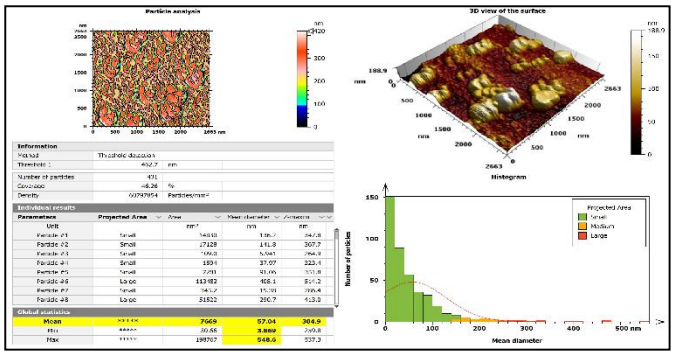

Figure 6. Particle AFM results

Transmission Electron Microscopy (TEM) and particle size distribution

Figure 7 shows the transmission electron microscopy (TEM) images of the synthesized nano copolymer. The images confirm that the copolymer nanoparticles exhibit an average particle size of approximately 57.48 nm, consistent with the results obtained from XRD and AFM analyses. The nanoparticles were observed in a variety of shapes, including spherical, discoid, cyclic, crystalline, and semi-spherical forms, indicating structural diversity and possible flexibility in molecular arrangement.

The TEM micrographs captured under both low and high magnification reveal a fairly uniform particle size distribution and smooth surface morphology, further supporting the successful formation of nanoscale particles.

Table 2 presents a detailed quantitative analysis of the particle size, angles, areas, and standard deviations obtained using ImageJ software. This data provides statistical validation for the observed dimensions and shape variations.

Figure 8 illustrates the histogram representing the frequency distribution of particle sizes. The histogram confirms a relatively narrow size distribution, centered around the mean diameter, supporting the conclusion that the synthesis yielded well-defined and consistently sized nanoparticles suitable for drug delivery applications.

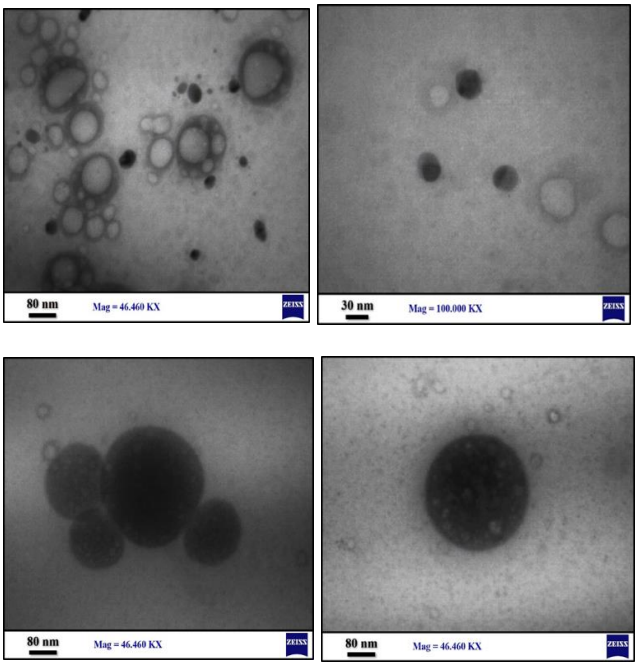

Figure 7. TEM micrographs of nanoparticle's copolymer

Table 2. Proportions diameters, angels and standard deviations of nano polymer

Area	StdDev	Angle	Diameter (nm)	D(av.) nm
13.667	10.551	43.668	40.552	**57.48**
18.889	8.639	118.989	56.399	
26.111	10.3	91.958	78.046	
15.444	13.99	2.49	46.043	
82	9.659	80.838	80.3	
80	7.232	83.418	78.518	
76	10.278	92.291	75.06	
67	7	95.194	66.272	
43	13.368	94.086	42.107	
80	7.568	26.565	70.01	
46	10.536	24.905	45.019	
3.667	9.511	-34.695	10.541	
93	6.326	-101.31	55.2	
73	17.612	56.976	71.561	
75	3.762	31.759	74.095	
56	7.646	40.601	55.317	
65	11.335	82.405	66.134	

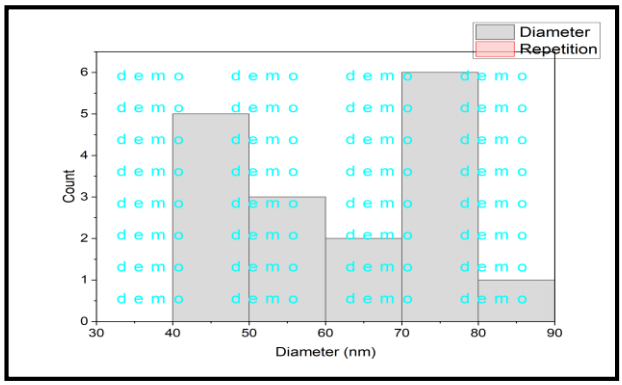

Figure 8. Histogram of different proportions of the particle sizes distribution

Synthesis of a nano drug composite

Reaction was carried out according to the following equation:

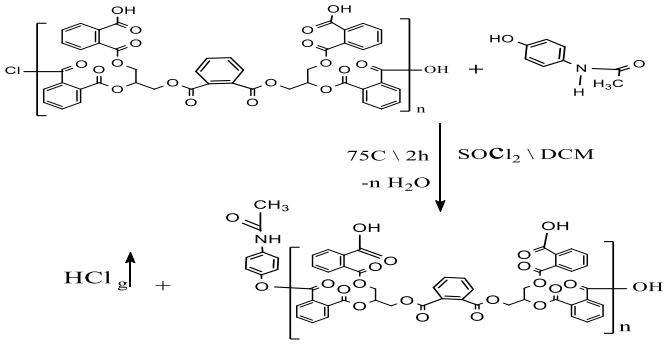

Equation 3. Synthesis of nano drug composite

Product yield equal 72%, m.p. 228 Co, FT-IR (KBr, cm-1): v 3323 (NH), 2600-3400 (OH), 2962 and 2874 (CH, sp3), 3084 (CH, sp2 of aromatic rings), 1609 bend (NH), 1434 (bend of CH2), 1766 (polymeric ester, C=O), 1705 (polymeric carboxyl, C=O), 1659 (carbonyl of secondary amide), Figure (3-8)

1H NMR (400 MHz, DMSO-d6); The single pick visible in 9.15 ppm for the OH to the drug amide group, signals from 7.70 to 6.35 ppm for the protons of the polymeric aromatic rings, quintet at 4.28-4.24 ppm for the protons of carbon 10 & 30, doublet at 3.76-3.67 ppm for the protons of carbon 11 & 9 , doublet at 3.61-3.59 ppm for the protons of carbon 29 & 30 and singlet at 1.98 ppm for carbon 69 & 81 . Figure (3-9).

13C NMR (101 MHz, DMSO-d6) δ peak at 169.13 for Carboxylic acid carbon 167.67 for carbon esters RCOOR , 165.80 ppm for imide carbon RCONHR - RCONH2R - RCONH2, 145.54 ppm to 115.45 ppm for carbon The carbon of the aromatic benzene ring , 80.42 ppm for carbon CHO, 65.95 ppm for carbon CHO 24.19 ppm for carbon CH3. Figure (3-10).

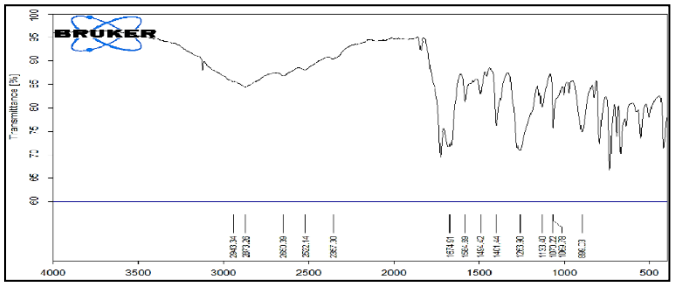

Figure 9. FT-IR spectrum of nano drug composite

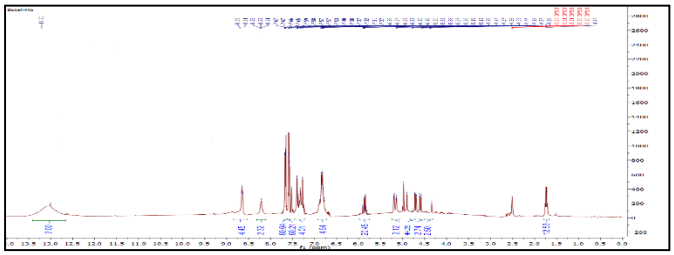

Figure 10. ^{1}H-NMR spectrum of nano drug composite

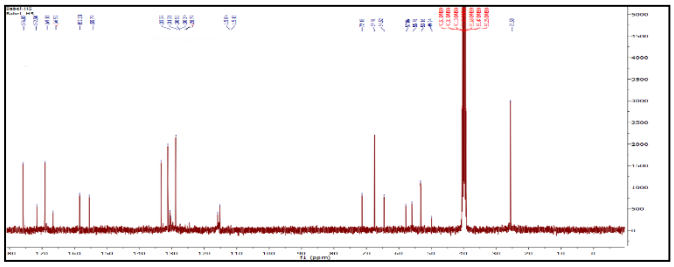

Figure 11. 13C-NMR spectrum of nano drug composite

Molecular docking of the drug composite

In Table 4, the results of molecular docking of the nano drug complex containing paracetamol (H3) with the target protein chain (PDB ID: 7zav), It is illustrated including the calculated binding energies and root mean square deviation (RMSD) values. These parameters allow excellent insight into the affinity, docking, and stability of the drug-protein complex.

Figure 12 illustrates the docking interaction between the nano composite drug and the amino acid cell cancer residues of the 7zav protein. Notably, leucine

(LEU, A:191) formed π-alkyl interactions with the drug, indicated in light purple. These hydrophobic interactions contribute significantly to the binding stability.

visualized in red is A repulsive interaction was observed between the electron-rich regions of the drug molecule & Serine(ser, A:172) and proline (PRO , A:175) , suggesting a potential steric or electronic hindrance at the site.

Several colored dark green is hydrogen bonds were identified between the drug of the polymer and key polar amino acid residues including Valine (VAL, A:176), glutamine (Glu, A:142), aspartic acid (Asp, A:168), and Phenylanine (PHE, A:143). These interactions play a crucial role in the specificity and strength of the ligand–receptor binding.

Additionally, C–H bonds (light green) were observed with proline (A:194) and valine (Ser, A:179). The remaining amino acids—phenylalanine (Phe), arginine (Arg), asparagine (Asn), methionine (Met), leucine (Leu), and glutamine (Gln)—contributed to van der Waals interactions, providing further stabilization to the complex.

Figure 13 presents the types and lengths of all molecular bonds formed between Paracetemol and the amino acids of the 7zav protein. Figure 14 highlights the specific regions where hydrogen bonding occurs, indicating critical areas of drug–target interaction.

These findings suggest that the nano drug composite forms multiple strong and specific interactions with the breast cancer-related protein, supporting its potential effectiveness as a therapeutic agent.

Table 4. Binding energy of drug composite (H3) with amino acids

Ligand	Binding Affinity (kcal/mol)	Mode	RMSD lower bound	RMSD upper bound
7zav_21_uff_E=945.59	-6.4	0	0.0	0.0
7zav_21_uff_E=945.59	-6.3	1	57.807	62.461
7zav_21_uff_E=945.59	-6.3	2	60.299	64.03
7zav_21_uff_E=945.59	-6.2	3	61.019	65.079
7zav_21_uff_E=945.59	-6.1	4	60.374	65.308
7zav_21_uff_E=945.59	-5.7	5	57.556	62.714
7zav_21_uff_E=945.59	-5.7	6	57.693	60.72
7zav_21_uff_E=945.59	-5.7	7	61.608	66.505
7zav_21_uff_E=945.59	-5.6	8	58.153	62.984

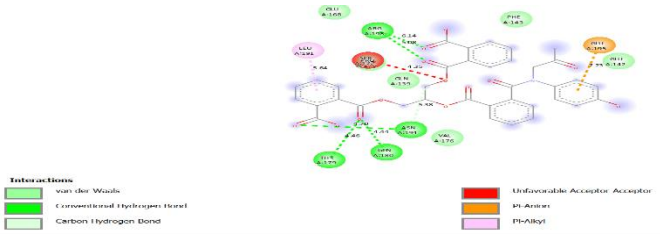

Figure 12. Bonds formed between the protein of cancer cells and the drug composite

Also given according to the donor part and the acquired part according to the figures below (13). The drug Paracetemol appears to be polymer-linked to the amino acids in the breast cancer protein.

And given according to the basic part and the acidic part also according to the figure below (14 donor). The cohesion of the drug Paracetemol bound to the polymer appears with the amino acids found in the breast cancer protein according to the acidic and basic groups.

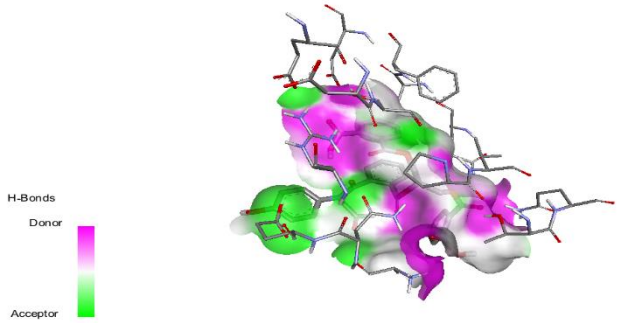

Figure 13. Binding of the drug (H3) bound to the protein of cancer cells.

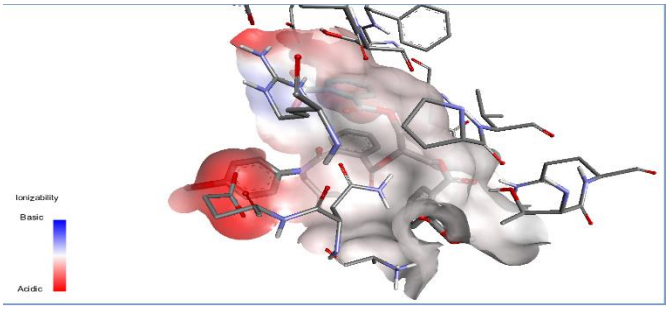

Figure 14. Binding of the drug composite (H3) bound to the protein of cancer cells.

The potential of nanocopolymer as an inhibitor of cancer cells, especially liver cancer cell lines as in the

sample, is closely related to its hydrogen bonding ability [16]. Hydrogen bonding enhances its biological activity by promoting stronger interactions with target enzymes in cancer cells, improving cell permeability, causing cancer cell death, and increasing selectivity toward cancer cells. The development of derivatives with hydrogen-bonding properties such as improved polymer nano composites could lead to more effective and safer anti-cancer therapies [27, 28].

Anti-cancer measurements

The anti-cancer potential of the prepared formulation was assessed against MCF-7 breast cancer cells. To measure the effectiveness of the drug in inhibiting cancer cells Figure 15A, we observe the form, that is, where the sample is untreated, we notice in it a large number of black dots that indicate cancer cells. However, in Model Figure15 B, the sample is treated with the polymer loaded with the drug, and we notice a significant inhibition in the cancer cells, as the black dots decrease significantly.

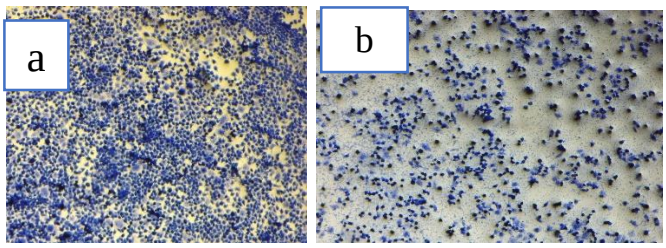

Figure (15). Picture represent; untreated cancer cells (a), treated cancer cells (b)

The cytotoxicity profile of H3 (Figure 16) revealed a clear dose-dependent inhibition of MCF-7 cell proliferation, with an IC50=52.46 µg/ml, demonstrating strong anti-proliferative activity. These findings are consistent with previous reports [29], where untreated cells appeared densely packed with irregular shapes and no swelling.

Post-treatment morphology in this study also mirrors earlier observations [30], showing a substantial decrease in cell number, distorted and swollen cells, and the appearance of dark spots indicative of debris from lysed cells. Such morphological changes strongly support the cytotoxic and cell-destructive effects of(H3) on MCF-7 breast cancer cells.

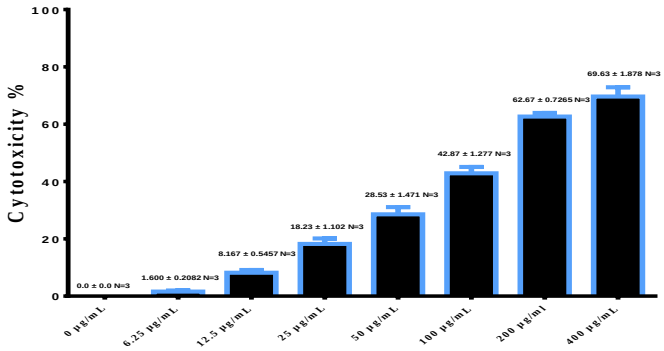

Figure 16. Cytotoxicity effect of H3 in MCF-7 cells. Data are represented as mean±SD. IC50=52.46 µg/ml

Figure 17. Cytotoxicity effect of H5 in MCF-7 cells. Data are represented as mean ± SD. IC50=55.09 µg/ml

Conclusion

A deep dive into the physicochemical landscape was undertaken, employing a suite of techniques including FT-IR, NMR, XRD, TEM, and AFM. The results painted a vivid picture of not just successful synthesis but also the thoughtful nano structuring of the polymer. Here, the average crystal size nestled neatly at 57.6 nm, while the d-spacing measured an intriguing 0.569 nm, accompanied by a surface roughness that stood at 29.72 nm. Such precise measurements whisper tales of a meticulously crafted nano-architecture. And here's the magic: these nanoscale attributes directly contribute to the material's prowess as a drug delivery carrier. In doing so, they bolster the physicochemical stability, elevate solubility, and enhance the biological performance of Paracetamol, seamlessly intertwining science and innovation.

Hydrogen bonding interactions with target biomolecules in cancer cells were identified as a critical factor in its anticancer efficacy. The engineered nano-carrier provided precise breast cancer cell targeting, increasing therapeutic selectivity and minimizing undesirable off-target effects. Such targeted delivery mechanisms are particularly valuable in oncology, where collateral damage to healthy cells often limits treatment effectiveness.

Biological evaluation through in vitro assays against the MCF-7 breast cancer cell line demonstrated potent anti-proliferative activity, with an IC50=52.46

μg/ml. Microscopic analyses revealed distinct morphological alterations, including cell shrinkage, membrane damage, and the formation of dark spots corresponding to lysed cellular debris, further validating its cytotoxic potential.

Beyond anticancer performance, the nano-engineered carrier offered significant pharmaceutical advantages. It improved drug stability, enhanced bioavailability, and protected amoxicillin from enzymatic degradation, thereby prolonging its therapeutic activity. These improvements collectively address key challenges in drug delivery systems, such as rapid drug clearance, low solubility, and systemic toxicity.

The present findings not only establish the promise of nano-engineered antibiotics in breast cancer therapy but also open new avenues for the repurposing of existing drugs through nanotechnology-based modifications. Future studies should focus on in vivo evaluations, long-term toxicity assessments, and potential combination therapies to fully realize the clinical potential of such systems. By bridging pharmaceutical nanotechnology with oncology, this approach represents a step forward in developing safer, more effective, and targeted cancer treatments.

Future Outlook

Building on these promising in vitro results, future research should prioritize comprehensive in vivo studies to evaluate the safety, pharmacokinetics, and therapeutic efficacy of the nano-engineered amoxicillin formulation. Long-term toxicity assessments will be critical to ensure biocompatibility and minimize adverse effects. Moreover, exploring combination therapies with other anticancer agents could enhance treatment outcomes through synergistic mechanisms.

Advancements in nanotechnology offer exciting opportunities to repurpose existing antibiotics, expanding their applications beyond infectious diseases to targeted cancer therapies. Continued optimization of nanocarrier design, including surface functionalization for improved targeting and controlled drug release, will further enhance clinical potential.

Ultimately, integrating such nano-engineered drug delivery systems into standard oncology protocols may significantly improve patient outcomes by providing safer, more selective, and effective cancer treatments. This study lays a strong foundation for the development of next-generation nanomedicines that harness the versatility of antibiotics for innovative cancer therapy.

Data Availability

All data have been given in the article and Supplementary Information.

References

1. Ab, K. I., Abbas, A. H., Abed, A. S., & Bahjat AL-Baiati, M. N. (2022). Nano-Poly Chitosan-Ampicillin Drug: Synthesis, Characterization and Cytotoxicity. *Egyptian Journal of Chemistry, 65*(131), 1313–1318. https://doi.org/10.21608/ejchem.2022.150425.6518
2. Abdulnabi, O., Alsalame, H., & Al-Baiati, M. (2024). Studying of Using Chitosan-Cephalexin Nano composed to Induce ROS and Apoptosis in Colon Cancer Cell Line HCT-29. *Moroccan Journal of Chemistry, 12*(3), 1270–1280. https://doi.org/10.48317/IMIST.PRSM/morjchem-v12i3.48702
3. Abdulridha, A. A., Abdul-Rida, N. A., & Al-Baiati, M. N. (2023). Synthesis of novel nano co-polymer as pH sensitive drug delivery system: Experimental and theoretical study. In *AIP Conference Proceedings* (Vol. 2414, No. 1). AIP Publishing. https://doi.org/10.1063/5.0114487
4. Abdulridha, A. A., Abdul-Rida, N. A., & Al-Baiati, M. N. (2023). Controlled drug delivery and release by new nanopolymer: Experimental and theoretical study. In *AIP Conference Proceedings* (Vol. 2414, No. 1). AIP Publishing. https://doi.org/10.1063/5.0114490
5. Al-Aama, Z. M. A., AL-Masoudi, H. Q., Abdulridha, A. A., Abd Nusaif, K. I., & Al-Baiati, M. N. (2023).

Synthesis of a smart nano graft co-polymer as a drug delivery. In *AIP Conference Proceedings* (Vol. 2414, No. 1). AIP Publishing. https://doi.org/10.1063/5.0114726

6. Khudhair, A. R., Sherazi, S. T. H., & Al-Baiati, M. N. (2020). Adsorption of methylene blue from aqueous solutions by using a novel nano co-polymer. In *AIP Conference Proceedings* (Vol. 2290, No. 1). AIP Publishing. https://doi.org/10.1063/5.0027741
7. Athab, A. H., Al-Safy, A. H., & Al-Baiati, M. N. (2022). Study of the effective range of drug level using a novel nano co-polymer–mefenamic acid. *International Journal of Drug Delivery Technology, 12*(4), 1808–1813. https://doi.org/10.25258/ijddt.12.4.53
8. Abd, K. I., & Ali, H. A. (2020). Identifying the LBP and insulin resistance: Potential role for the increased feto-maternal morbidity and long-term complications. *Biochemical & Cellular Archives, 20*(2).
9. Abd N., K. I., Sara, A. M., & Inam, J. R. (2024). Association between sex hormonal and metabolic changes in females with infertility in Al-Najaf city patients. *Ginekologia i Położnictwo, 68*(4), 1–5.
10. Al-Ghanimi, B., Abd Nusaif, K., & Al-Baiati, M. (2025). Novel nano chitosan loaded with amoxicillin as inhibitor of lung cancer cell line (A549): Biological activity and molecular studies. *Moroccan Journal of Chemistry, 13*(2), 480–494. https://doi.org/10.48317/IMIST.PRSM/morjchem-v13i2.49619
11. Shakir, Z. M., Kareem, M. M., & Al-Baiati, M. N. (2023). Inhibition of spread of breast cancer by using some nano co-polymer-drugs. In *AIP Conference Proceedings* (Vol. 2414, No. 1). AIP Publishing. https://doi.org/10.1063/5.0114719
12. Anad, M. F., Salman, H. E., & Al-Baiati, M. N. (2019). Synthesis of a novel nano graft co-polymer and studying the swelling behaviors using different molar ratios of acrylic acid monomer. *IOP Conference Series: Materials Science and Engineering, 571*(1), 012096. https://doi.org/10.1088/1757-899X/571/1/012096
13. Al-Baiati, M. N., Jafar, N. N., & Zaooly, R. H. (2016). Study the effect verifies of the number of moles of acrylic acid monomer on swelling of the newly prepared modified co-polymer. *Research Journal of Pharmaceutical, Biological and Chemical Sciences, 7*(5), 1452–1463.
14. Abdulnabi, O., Alsalame, H., & Al-Baiati, M. (2025). Preparation and characterization of nano chitosan–mefenamic acid composites as biocompatible treatment against colon cancer cell line HCT-29. *Moroccan Journal of Chemistry, 13*(1), 366–380. https://doi.org/10.48317/IMIST.PRSM/morjchem-v13i1.49451
15. Obaid, M. M., & Al-Baiati, M. N. (2023). Studying the effectiveness of using a novel nano polymer as a protein delivery system. In *AIP Conference Proceedings* (Vol. 2414, No. 1). AIP Publishing. https://doi.org/10.1063/5.0114723
16. Al-Ghanimi, B. K., Abd, K. I., Al-Baiati, M. N., Al-Ghanimi, H. H., & Al-Madany, R. A.-A. (2024). Using a novel nano chitosan ampicillin drug as a treatment for lung cancer cell line (A549). *Arabian Journal of Medicinal and Aromatic Plants, 10*(2), 1–21.
17. Hassan, S. F., Habeeb, Z. T., & Al-Baiati, M. N. (2025). Synthesis and characterization a novel nano co-polymer–drugs composites and using it as treatment to liver cancer. *Moroccan Journal of Chemistry, 13*(1), 106–121. https://doi.org/10.48317/IMIST.PRSM/morjchem-v13i1.50079
18. Shakir, Z. M., Kareem, M. M., & Al-Baiati, M. N. (2023). Study the effects of some nano graft co-polymer-drugs on the spread of breast cancer. In *AIP Conference Proceedings* (Vol. 2414, No. 1). AIP Publishing.

https://doi.org/10.1063/5.0114710
19. Xu, Q., Pan, H., Zhang, W., Xu, L., & Li, T. (2024). Preparation and photocatalytic performance of TiO_2/lignin-based carbon composited photocatalyst. *Journal of Physics: Conference Series, 2671*(1), 012013.
20. Huang, A., Zhou, Q., Liu, J., Fei, B., & Sun, S. (2008). Distinction of three wood species by Fourier transform infrared spectroscopy and two-dimensional correlation IR spectroscopy. *Journal of Molecular Structure, 883*, 160–166.
21. Wiese, L. (2024). Total synthesis of the antiviral natural products Cleistocaltone A and B.
22. Frank, A. F. (2025). The design, synthesis, and characterization of gallium-salophen complexes (GaSal-3) as inhibitors of *Pseudomonas aeruginosa* heme sensing and utilization system (Doctoral dissertation). University of Maryland, Baltimore.
23. Ma, C. Y., Xu, Y., Xu, L. H., Zhang, C., Qi, J. Y., & Wen, J. L. (2024). NMR characterization of lignin. In *Lignin Chemistry: Characterization, Isolation, and Valorization* (pp. 15–60).
24. Khachatryan, D. S., et al. (2025). Novel derivatives of thiohydantoin-containing tetrahydro-β-carboline possess activity against influenza virus at late stages of viral cycle without affecting viral neuraminidase. *Archiv der Pharmazie, 358*(3), e2400733.
25. Caruso, M. R., Cavallaro, G., Milioto, S., & Lazzara, G. (2023). Halloysite nanotubes/Keratin composites for wool treatment. *Applied Clay Science, 238*, 106930.
26. Monshi, A., Foroughi, M. R., & Monshi, M. R. (2012). Modified Scherrer equation to estimate more accurately nano-crystallite size using XRD. *World Journal of Nano Science and Engineering, 2*(3), 154–160.
27. Habeeb, Z. T., Ab, K. I., & Naser, M. S. (2022). Monitoring study on the incidence of 25-OH Vitamin D deficiency in population of Kerbala Province. *Egyptian Journal of Chemistry, 65*(131), 1319–1322. https://doi.org/10.21608/ejchem.2022.150424.6517
28. Khaldan, A., et al. (2021). Aspirin-loaded chitosan nanoparticles: A breakthrough in liver cancer therapy. *Heliyon, 7*(3), e06603. https://doi.org/10.1016/j.heliyon.2021.e06603
29. Hao, Y., et al. (2020). Exopolysaccharide from *Cryptococcus heimaeyensis* S20 induces autophagic cell death in non-small cell lung cancer cells via ROS/p38 and ROS/ERK signalling. *Cell Proliferation, 53*(8), e12869.
30. Jin, Y., et al. (2023). Hydroponic ginseng root mediated with CMC polymer-coated zinc oxide nanoparticles for cellular apoptosis via downregulation of BCL-2 gene expression in A549 lung cancer cell line. *Molecules, 28*(2), 906.
31. Mansoor, M., Jam, F. A., & Khan, T. I. (2025). Fostering eco-friendly behaviors in hospitality: engaging customers through green practices, social influence, and personal dynamics. International Journal of Contemporary Hospitality Management, 37(5), 1804-1826.